

4U 1957+11: a persistent low-mass X-ray binary and black-hole candidate in the high state?

Rudy Wijnands^{1*}, Jon M. Miller¹, Michiel van der Klis²

¹ Center for Space Research, MIT, NE80-6055, 77 Massachusetts Avenue, Cambridge, MA 02139-4307, USA

² Astronomical Institute “Anton Pannekoek”, University of Amsterdam, Kruislaan 403, NL-1098 SJ Amsterdam, The Netherlands

27 October 2018

ABSTRACT

We report on several pointed *Rossi X-ray Timing Explorer* observations of the enigmatic low-mass X-ray binary (LMXB) 4U 1957+11 at different X-ray luminosities. The luminosity of the source varied by more than a factor of four on time scales of months to years. The spectrum of the source tends to get harder when its luminosity increases. Only very weak (1%–2% rms amplitude; 0.001–10 Hz; 2–60 keV) rapid X-ray variability was observed during the observations. A comparison of the spectral and temporal behaviour of 4U1957+11 with other X-ray binary systems, in particular LMC X-3, indicates that 4U 1957+11 is likely to be a persistent LMXB harboring a black hole and which is persistently in the black-hole high state. If confirmed, it would be the only such system known.

Key words: accretion, accretion discs – stars: binaries: close – stars: individual: 4U 1957+11 – X-rays: stars

1 INTRODUCTION

Low-mass X-ray binaries (LMXBs) are systems in which a compact object (either a neutron star or a black hole) accretes matter from a low-mass ($<1 M_{\odot}$) companion star. Approximately 150 LMXBs are known (van Paradijs 1995; Liu, van Paradijs, van den Heuvel 2001) and for many of these systems the nature of the compact object could be uniquely identified as a neutron star based on the observation of thermonuclear flashes from the star’s surface (so-called type-I X-ray bursts) or from X-ray pulsations. For several LMXBs (all X-ray transients) the nature of the compact object was deduced to be a black hole based on the large mass-function (and consequently the large lower limit on the mass of the compact object) obtained from those systems when they were in their quiescent state (see, e.g., Filippenko et al. 1999 and McClintock et al. 2001 and references therein). For the remaining LMXBs the nature of the compact is still unknown. However, the possible nature is often deduced from similarities of those systems with LMXBs for which the nature of the primary could be determined. But neutron star and black-hole LMXBs are very similar with respect to their X-ray spectral (e.g., Barret & Vedrenne 1994; Barret et al. 1996) and X-ray timing properties (e.g., van der Klis 1994a, 1994b; Wijnands & van der Klis 1999) and classifications based on resemblances are difficult and subject to errors.

One of the persistent LMXBs for which the exact nature of the compact object is still a subject of debate is 4U 1957+11. Its soft X-ray spectrum led White & Marshall (1984) to suggest that 4U 1957+11 is a candidate to harbor a black hole (a black-hole candidate or BHC). However, such a soft spectrum is not a strong conclusive argument and can be interpreted in different ways. For example, the spectral studies reported in the literature both give evidence for a neutron star (*Ginga*: Yaqoob, Ebisawa, & Mitsuda 1993; *EXOSAT*: Singh, Apparao, & Kraft 1994) or a black hole (*EXOSAT*: Ricci, Israel, & Stella 1995) primary. The study performed by Nowak & Wilms (1999; using data obtained with the X-ray satellites *Rosat*, *ASCA*, and the *Rossi X-ray Timing Explorer* [*RXTE*]) showed that the spectrum of 4U 1957+11 can be understood in different ways and that the nature of the compact object remains elusive.

The optical counterpart of 4U 1957+11 (V1408 Aquilae) was discovered by Margon, Thorstensen, & Bowyer (1978) and its orbital period of 9.33 hr by Thorstensen (1987). Hakala, Muhli, & Dubus (1999) studied V1408 Aquilae in more detail and reported that the optical light curve pulse shape over the orbital period changed between their study and the study of Thorstensen (1987). They proposed that these changes are due to an evolving accretion disc structure. From their models a large inclination angle of 70° – 75° was obtained, which Nowak & Wilms (1999) combined with the 117 day period they reported in the *RXTE* All Sky Monitor (ASM) light curve of 4U 1957+11 to pro-

* Chandra Fellow; Email:rudy@space.mit.edu

pose that the X-ray spectrum and its variations are due to a warped precessing accretion disc.

In this paper, we present data of 4U 1957+11 obtained with the proportional counter array (PCA) on board *RXTE* when the source was at luminosities up to four times higher than during the observations reported by Nowak & Wilms (1999). We also analyzed a more extensive *RXTE*/ASM data set and conclude the long-term behaviour significantly changes with time. We discuss our spectral and timing results with respect to the nature of the compact object.

2 OBSERVATIONS

During Cycle 2 of *RXTE*, 4U 1957+11 was observed for ~ 29 ksec when the source was at low luminosities (Fig. 1; see also Nowak & Wilms 1999; hereafter referred to as the AO2 observations). To study the spectral and timing behaviour of this source at higher luminosity levels, we had proposed to perform Cycle 4 *RXTE* TOO observations on this source when its count rate would exceed 3 ASM counts s^{-1} . This programme was approved, and observations (hereafter referred to as the AO4 observations) were indeed triggered, resulting in a total of 38.6 ksec of data (see Table 1 for a log of the observations). We reanalyzed the AO2 data to obtain an homogeneous analysis for all observations.

During all observations data were collected in the Standard 1 (1/8 s time resolution in one photon energy channel for the energy range 2–60 keV) and the Standard2f (129 channels for 2–60 keV; 16 s time resolution) modes. Simultaneously, data were also collected during the AO2 data with the GoodXenon1.16s and GoodXenon2.16s modes (together they have 256 channels for 2–60 keV and a time resolution of $\sim 1 \mu\text{s}$). During the AO4 observations, data were collected in one event mode (E_125us_64M_0.1s: 128 μs time resolution in 64 channels from 2–60 keV), one single bit mode (SB_125us_0.249_1s: 128 μs time resolution in 1 channel from 2–60 keV), and a burst trigger (TLA_1s_10_249_1s_10000_F) and catcher (CB_8MS_64M_0_249_H) mode. The last three modes were active in order to study type-I X-ray bursts (the single bit mode for high time resolution and the catcher mode for high spectral resolution at modest time resolution) in case 4U 1957+11 should harbor a neutron star. However, no bursts were found and we do not discuss the data obtained in these modes further in our paper.

The five PCA detectors (called proportional counter units or PCUs) each have a slightly different energy response. Due to aging of the electrodes and processes as gas leakage, the gain of the individual detectors drifts slowly in time. More sudden changes in the gain are caused by changes in the high voltage settings (which are occasionally made in order to preserve the detectors), resulting in (so far) four major gain epochs. The AO2 observations and the first one of the AO4 observations (observation number 5 in Table 1) were taken during gain epoch 3 and the other observations during gain epoch 4. Not all of the five detectors were always on during our observations, resulting in a different number of active detectors (between 2 and 5, see Table 1) throughout our study.

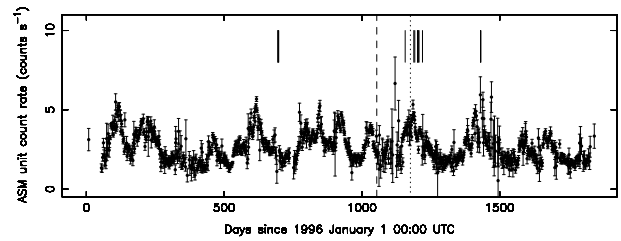


Figure 1. The 1.5–12 keV *RXTE*/ASM count rate curve in 2 days rebinning up to 18 January 2001. The solid lines correspond to the dates of the observations listed in Table 1 (the first line corresponds to the AO2 data and the others to the AO4 data). The dotted line marks the end of *RXTE*/PCA gain epoch 3 and the start of epoch 4. The data up to the dashed line was already presented by Nowak & Wilms (1999) and used in their analyze.

3 ANALYSIS AND RESULTS

3.1 The *RXTE*/ASM light curve

We used the quick-look one-day averaged *RXTE*/ASM data[†] of 4U 1957+11 in order to study its long-term variability. The resulting long-term ASM light curve of 4U 1957+11 is shown in Figure 1. The source smoothly varies between ~ 1 and ~ 6 ASM count s^{-1} , with clear episodes of low and high luminosities. In this figure, we have indicated when the pointed *RXTE* AO2 (first solid vertical line) and our AO4 observations (the other solid vertical lines) were performed. Clearly our strategy to observe 4U 1957+11 at high luminosities succeeded, resulting in 38.6 ksec of data during which the luminosity of the source was 2–4 times higher than during the AO2 observations.

Nowak & Wilms (1999) reported a 117 day period in the *RXTE*/ASM long-term X-ray light curve of 4U 1957+11. They used the available data up to 1998 November 20. Since then, a significantly larger data set has become available and therefore we decided to analyze all ASM data available up to the writing of this paper (2001 January 18). We made a Lomb-Scargle diagram (Lomb 1976; Scargle 1982) of the ASM data (see Fig. 2a). This figure clearly shows multiple peaks above 100 days. The most significant peak is the one at 250–260 days, but several other peaks between 100 and 400 days are also present. These peaks are in the range of the ones found by Nowak & Wilms, but they are not exactly similar. This could indicate that no complete stable period is present in the system.

In order to study this possibility, we made Lomb-Scargle diagrams of the data used by Nowak & Wilms (1999; up to 20 November 1998; Fig. 2b) and of the data taken after that (up to 18 January 2001; Fig. 2c). The 117 day peak is clearly the most significant in the first data set, however, in the second data set this peak is nearly absent but a dominant peak is present around 250 days. This result strongly suggest that the long-term variability behaviour of 4U 1957+11 is more complicated than suggested by the 117 day period reported by Nowak & Wilms (1999).

[†] the quick-look data can be obtained from http://xte.mit.edu/ASM_lc.html and is provided by the ASM/*RXTE* team. See Levine et al. (1996) for a detailed description of the ASM.

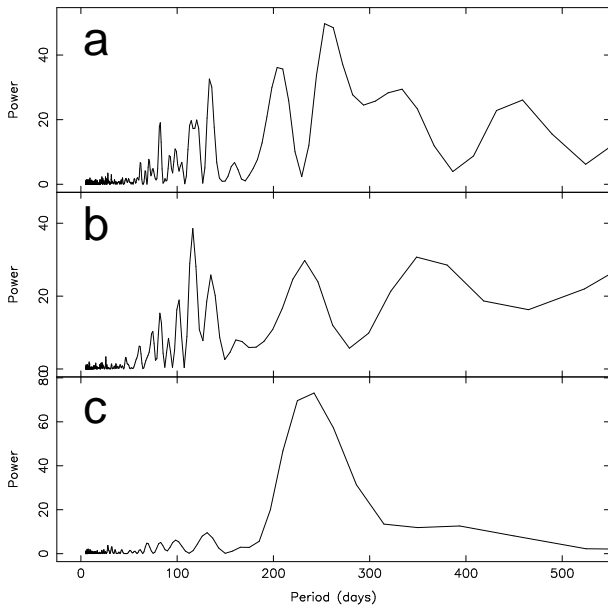


Figure 2. Lomb-Scargle diagrams for 4U 1957+11 of (a) all *RXTE*/ASM data available (up to 2001 January 18; using the light curve which was also used to make Figure 1), (b) the data used by Nowak & Wilms (1999; up to 1998 November 20), and (c) the data obtained between 1998 November 20 and 2001 January 18.

3.2 The *RXTE*/PCA light curve

We used the Standard2f data in order to create a *RXTE*/PCA light curve for the total *RXTE*/PCA energy range of 2–60 keV (see Fig. 3a). The count rates were background subtracted but no dead-time correction was applied. However, we estimate that the correction factor would be $<0.5\%$, which is considerably smaller than the errors on the count rates due to counting statistics. From Figure 3a and from Table 1, it can be seen that we have obtained *RXTE*/PCA data of 4U 1957+11 at a count rate which is up to 4 times higher than its count rate observed during the AO2 observations. This allows us to study the 3–20 keV X-ray spectrum and the rapid X-ray variability of this source at different luminosities.

The count rates during the individual observations vary only slightly (typically between 5%–15%). However, one observation (observation 6) behaved differently. In Figure 3b, the PCA light curve of this observation is shown. At the beginning of the observation, the source was at ~ 85 counts s^{-1} PCU $^{-1}$, but it steadily increased with time. Due to an occultation of the source by the Earth, the data are interrupted. However, when the source could be observed again with *RXTE*, it was clear that the count rate increase had continued. This continuation can still be seen in beginning of the second data set in Figure 3b. The source then reached its highest count rate (~ 165 counts s^{-1} PCU $^{-1}$) at which approximately level it stayed for the remainder of the observation. Similar behaviour was not observed during the other observations. Hereafter, we refer to the rising part of this observation as ‘the rise’ or observation 6a, and to the rest as ‘the plateau’ or observation 6b.

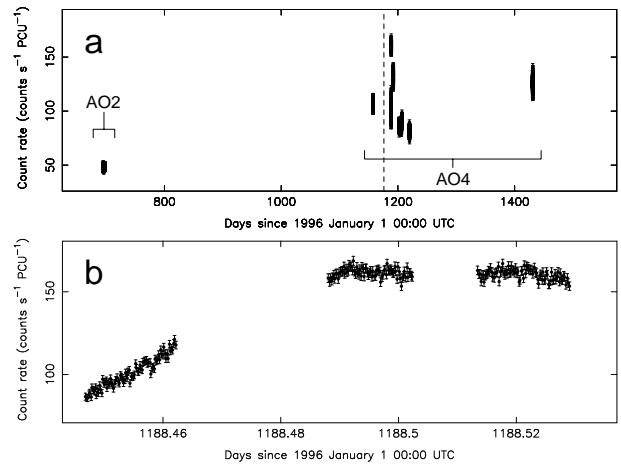


Figure 3. The 2–60 keV *RXTE*/PCA count rate curves, with (a) the total count rate curve and (b) a blow up of observation 40044-01-02-01 (observation 6) showing the rising phase and the plateau. The count rates are background subtracted but not dead-time corrected ($<0.5\%$). The dashed line in (a) indicates when the high voltages of the PCUs were changed and marks the end of gain epoch 3 and the start of gain epoch 4.

3.3 The rapid X-ray variability

We made power spectra, using 16 s data segments, of the combined GoodXenon mode data of the AO2 observations and of the AO4 event mode data in order to study the X-ray fluctuations. No significant rapid X-ray variability was observed in the individual observations for frequencies above 0.1 Hz, with typical rms amplitude upper limits of 1%–3% on a power-law noise component with index 1 (for the 2–60 keV energy range and a 0.1–10 Hz frequency range). These limits are consistent with what has been measured by Nowak & Wilms (1999) using only the AO2 data. In order to study the variability at lower frequencies (a possible very-low frequency noise component or VLFN), we also made power spectra using 1024 s data segments. Again, only upper limits could be determined for most observations, except for observation 6a during which a band-limited noise component was present. Although the statistics did not allow for constraints on the exact shape of this noise component, we fitted it with a power-law. The fit parameters obtained are listed in Table 2. The noise during this observation was significantly stronger ($\sim 6\%$ rms; 0.001–10 Hz) than the upper limits (95% confidence levels) obtained for the other observations (typically a few percent), in particular for observation 6b which followed observation 6a immediately. However, this strong noise during observation 6a is very likely caused by the rising trend in this observation.

In order to improve our sensitivity for VLFN we combined all the AO4 observations together (except observation 6) to see if a VLFN component is present below 0.1 Hz. The resulting power spectrum is shown in Figure 4a. We indeed detect a VLFN with a rms amplitude of $1.82\% \pm 0.07\%$ (0.001–10 Hz; 2–60 keV) and an index of 1.36 ± 0.07 . For a source as weak as 4U 1957+11, part (if not all) of the observed variability might be due to the fluctuations in the background. To investigate this possibility, we made similar power spectra of a large number of *RXTE*/PCA background

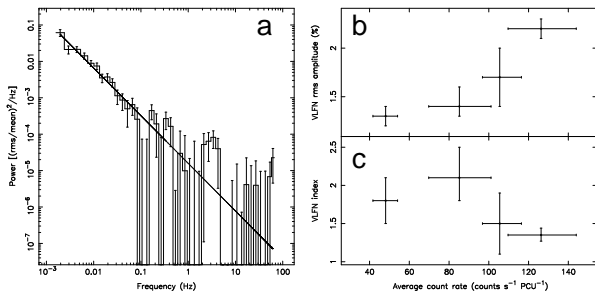


Figure 4. (a) Power spectrum of all the AO4 observations combined (except observation 6). The Poisson level has been subtracted. The VLFN rms amplitude is $1.82\% \pm 0.07\%$ (0.001–10 Hz; 2–60 keV) and the VLFN index 1.36 ± 0.07 . (b) the VLFN rms amplitude measured over the frequency range 0.001–10 Hz and (c) the VLFN index versus the average 2–60 keV count rate.

observations performed near the dates of our 4U 1957+11 observations. A power-law shaped noise component was indeed detected with an rms amplitude of 1%–2%. Although this noise is of similar strength as the VLFN noise component in 4U 1957+11, its index (~ 2) is considerably larger than that observed for 4U 1957+11. Furthermore, a large amount of extra source counts are present in the 4U 1957+11 and if all the variability observed for 4U 1957+11 would have been only due to background fluctuations then the observed strength of the VLFN component should be weaker than we observe. Therefore, we conclude that at least part of the observed variability is due to intrinsic variability of 4U 1957+11.

In order to determine if the strength and the steepness of this noise component are correlated with the count rate, we combined only those observations which had approximately similar count rates. We obtained four count rate intervals and we could detect the VLFN in all of these selections (see Tab. 2). Note that we did not use observation 6 in this analysis because of the unusual behaviour of 4U 1957+11 during this observation compared to the other observations. The rms amplitude and the index of the VLFN are plotted in Figures 4b and 4c versus the average count rate of the selection. The range in count rate observed during the observations which were combined, served as an error on the count rates. This is a rather conservative error and causes the error bars on the average count rate to overlap in Figure 4b and 4c. Yet, a clear trend is visible in that the strength of the VLFN increased with increasing count rate. As explained above, not all the observed variability of 4U 1957+11 can be due to background fluctuations. The fact that we observe the strongest variability when the source is brightest, is also consistent with this interpretation (if the background was the dominant source of the variability, it would be expected that the strength would decrease with count rate as more and more source counts are added). However, at the lowest count rate selections, it is possible that most of the variability is due to background fluctuations, but this will only make the trend in Figure 4b more apparent. The fact that the VLFN index seems to increase when the count rate decreases also indicates that the variability becomes background dominated at the lowest count rates.

From Figure 4b it is also clear that observation 6 does

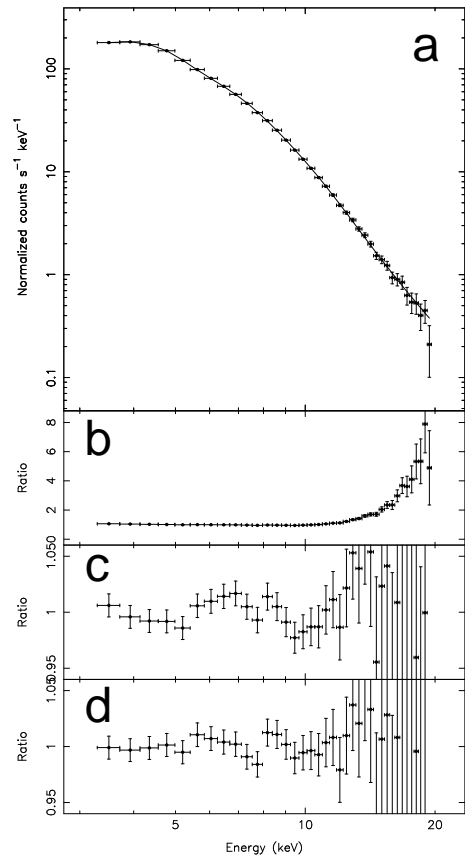


Figure 5. A typical spectrum of 4U 1957+11 (a; observation 11). The ratio of the spectrum with a fit consisting of a multi-colour disc model (b), a multi-colour disc plus power-law model (c), and a multi-colour disc plus power-law model and including a line at 6.5 keV (d).

not follow the trend. During the rise part of this observation the average count rate was ~ 101 counts s^{-1} PCU $^{-1}$ but the VLFN strength was $\sim 6\%$ rms, considerably stronger than expected from this correlation. We note again that this strong VLFN component is very likely due to the rising trend. However during the plateau phase of this observation the upper limit (95% confidence level) on a VLFN component was only 1.1% rms which was lower than expected from this correlation. Clearly, during observation 6, 4U 1957+11 behaved quite differently compared to its behaviour during the other observations.

3.4 The X-ray spectra

We extracted the spectral data obtained in the Standard2f mode to investigate the spectral characteristics of 4U 1957+11 in each observation. Due to the variable number of active detectors and to obtain the fullest spectral response, we chose to fit the data from all layers of all active PCUs in each observation. Background subtraction and the creation of response matrices were accomplished using the tools available through LHEASOFT version 5.0 (“pcabackest” using

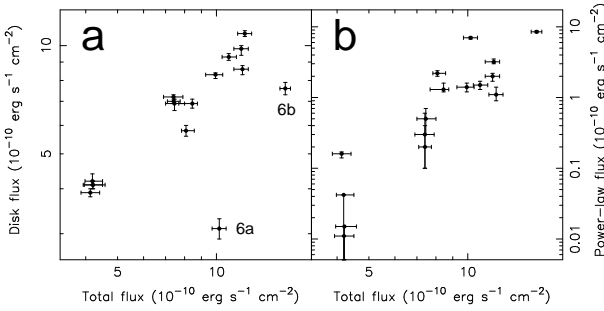


Figure 6. The disc flux versus the total unabsorbed flux (a) and the power-law flux versus the total unabsorbed flux (b). The fluxes are for 3–20 keV. The two data points labeled with 6a and 6b are the data points corresponding to observations 6a and 6b, respectively (see Tab. 1).

the “bright source” background model, and “pcarsp,” respectively). Fits to an observation of the Crab (nearly a pure power-law at PCA resolution) made near to the time of the AO4 observations of 4U 1957+11 indicate that the response matrices perform well above 3 keV, and we therefore adopt this as the lower bound on our fitting range. Those fits also show energy dependent residuals which can be as large as 1.0%; we therefore add 1% systematic errors when fitting data from 4U 1957+11 (this has become standard in fitting PCA data, see, e.g., Miller et al. 2001, McClintock et al. 2001). We adopt 20 keV as an upper bound for our fits to 4U 1957+11, as the spectrum is background-dominated above this energy. As the *RXTE*/PCA is not very sensitive to the absorption column towards 4U 1957+11, we fixed the N_{H} to 1.3×10^{21} atoms cm^{-2} (Dickey & Lockman 1990). Errors on the fit parameters were calculated for 90% confidence.

The X-ray spectra of LMXBs and of 4U 1957+11 in particular can be fit with a variety of models (e.g., Christian & Swank 1997; Nowak & Wilms 1999). However, 4U 1957+11 is a potential BHC and the X-ray spectra of these sources are usually fitted with a two-component model: a multi-colour disc black-body (MCD) and a power-law. A similar consensus is not present for the models for neutron-star systems. Therefore, we only use the MCD plus power-law model for 4U 1957+11. If this source contains a neutron star, we might obtain unusual results using this model.

Our fits to the Crab data shows a slight excess near 6 keV with an equivalent width (EW) of about 40–60 eV. In order to obtain acceptable fits, we also included a line in our 4U 1957+11 spectral fits with a fixed energy of 6.5 keV. The obtained EWs of these lines are considerably larger than 40–60 eV (see Tab. 3), which suggest that a line or a complex of lines might be present around 6.5 keV. Including the line, the fit had 39 degrees of freedom (41 without line). The reduced χ^2 of the fits were below (but near) 1 except for observations 1 and 2 where they were ~ 1.7 . A typical spectrum of 4U 1957+11 is shown in Figure 5a (see also Nowak & Wilms 1999 for another spectrum of 4U 1957+11, but without a power law) and the fit parameters are listed in Table 3.

From Figure 5b–d it is clear that a power-law component was required in most observations (except for the AO2 observations; upper limits on the flux from a possible power-law

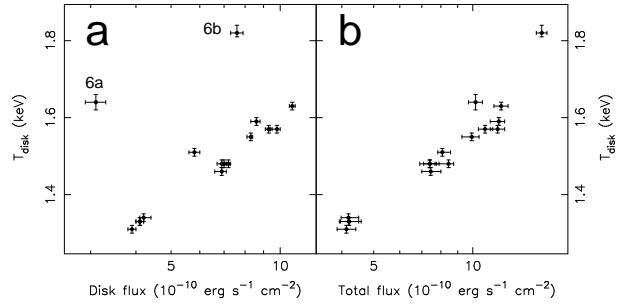


Figure 7. The disc temperature versus (a) the disc flux and (b) the total unabsorbed flux. The fluxes are for 3–20 keV. The two data points labeled with 6a and 6b are the data points corresponding to observations 6a and 6b, respectively (see Tab. 1).

component were obtained by fixing the power-law index to 2.5) and that the addition of a line at 6.5 keV also improved the fit (in this particular instance the reduced χ^2 decreased from 2.1 without the line to 0.4 with the line). Some results of the fits are plotted in Figure 6 and 7. From Figure 6a it is clear that, when not taking observation 6 into account, the disc flux steadily increases with the total unabsorbed flux. It is also clearly visible that the data of observation 6 (both the rise and the plateau part) are significantly below this correlation. In Figure 6b, it can be seen that the flux in the power-law tends to increase when the overall flux increases, and the data during observation 6 have the largest power-law fluxes. Only in this observation the power-law flux equals the disc flux, but for the other observations the power-law flux/disc flux ratio is well below 0.5. Interesting is also the correlation between the temperature of the disc with the disc flux (Figure 7). The temperature is correlated with the disc flux except again for the data obtained during observation 6. However, when using the total unabsorbed flux instead of the disc flux, the data of observation 6 line up much better.

3.5 The X-ray colours

We made a colour-colour diagram (CD; Fig. 8a) and hardness-intensity diagrams (HIDs; Figs. 8b and c) using the AO4 Standard2f data (except for observation 5). We used only the data of the two detectors (PCUs 0 and 2) which were always active. The colours used to produce these diagrams are listed in the caption of Figure 8. Note that both colours have the same soft band. This was done to ensure the linearity of the CD: any linear combination of two spectral models lies on the straight-line segment connecting their locations in the CD (see Belloni et al. 2000 and Homan et al. 2001 for this procedure). In the CD, the lines of a pure black-body spectrum and a pure power-law spectrum are included. The AO2 data and observation 5 were obtained during gain epoch 3 and the other observations during epoch 4. Due to the different responses of the PCUs during each epoch, the CDs obtained for each epoch cannot be compared directly with each other. We do not show the epoch 3 CD because the AO2 data all fall in the same place and the long-term gain drift in the PCUs make it difficult to compare observation 5 with the AO2 data.

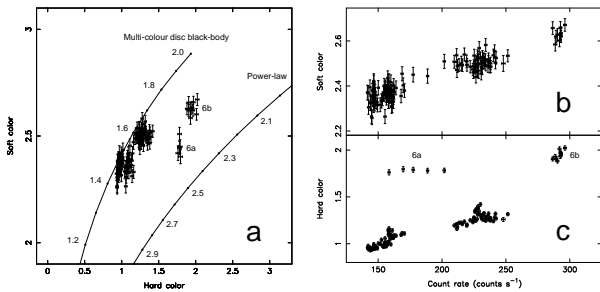


Figure 8. (a) Colour-colour diagram, (b) soft hardness-intensity diagram, and (c) hard hardness-intensity diagram of 4U 1957+11. The count rate is for 2.9–16.2 keV and 2 detectors. The soft colour is the count rate ratio between 3.7–6.3 keV and 2.9–3.7 keV, and the hard colour the one between 6.3–16.2 keV and 2.9–3.7 keV. The lines in (a) indicate the colours a pure multi-colour disc black-body or a pure power-law would have (assuming a column density of 1.3×10^{21} atoms cm^{-2}). In (a) and (c), the data points corresponding to observation 6a and 6b are indicated. The count rates used to produce these figures were background subtracted.

From Figure 8a it is clear that, except for observation 6, the source spectra are dominated by the MCD component with only little contribution of the power-law component. The evolution (i.e., hardening) of the source spectra during observation 6 is mainly due to the increase of the temperature of the MCD component, but with a significant contribution of an decrease of the power-law index. All these features are in good accordance with the results obtained via the spectral fits (section 3.4, Tab. 3). The soft colour and the hard colour (except observation 6) are also well correlated with the count rate (Fig. 8b and c). The hard colour for observation 6a is significantly larger than during the other observations with similar count rates. It is unclear whether the hard colours of observation 6b are correlated in the same manner with the count rate as the hard colours of the other observations, or that this observation by chance lines up with the other observations. From Fig. 8c it can also be seen that the hard colours during the other observations are not always completely correlated with the count rate; small excursions to higher hard colours at the same count rates can be observed.

4 THE DISTANCE TO 4U 1957+11

Margon et al. (1978) estimated the distance to 4U 1957+11 to be 7 kpc. They obtained this distance estimate by comparing the optical and X-ray properties of 4U 1957+11 to that of the bright neutron star LMXB Sco X-1. Although a valid method at the time, nowadays it is clear that Sco X-1 and 4U 1957+11 are likely different kinds of objects and a direct comparison of their properties will likely produce invalid results. Moreover, Margon et al. (1978) used an assumed distance to Sco X-1 of only 500 pc. However, recent high-resolution parallax measurements of Sco X-1 showed that the most likely distance to this source is 2.8 ± 0.3 kpc (Bradshaw, Fomalont, & Geldzahler 1999). Following the reasoning of Margon et al. (1978) this revised distance would result in a new distance estimate of 29 kpc for 4U 1957+11. This distance seems highly unlikely demonstrating that Sco X-1

and 4U 1957+11 are indeed different types of objects. Therefore, we regard the distance to 4U 1957+11 as unknown. We note however that this does not mean that we assume that 4U 1957+11 is further away than 7 kpc and thus more luminous than previous thought. In fact the source might be much closer and might be less luminous than 10^{36-37} erg s^{-1} .

5 DISCUSSION

We have observed 4U 1957+11 at a variety of X-ray luminosities (using both the *RXTE*/ASM and PCA data) and studied its spectral and temporal behaviour at those different luminosities. We first compare our results with those obtained previously for 4U 1957+11 and then with other LMXBs.

5.1 Comparison with other 4U 1957+11 observations

Our spectral results for 4U 1957+11 agree very well with those listed in the literature for this source (e.g., Yaqoob et al. 1993; Ricci et al. 1995; Nowak & Wilms 1999). In particular, the same hardening of the source spectrum we see with increasing flux had already been found earlier (e.g., Yaqoob et al. 1993; Ricci et al. 1995). Yaqoob et al. (1993) even found the same small excursion of the source in the HID towards harder colours at the same intensity as we do (e.g., compare their Figure 2 with our Figure 8; here we do not mean the enigmatic behaviour of observation 6, but the very small excursions in the HID mentioned at the end of section 3.5). The lack of rapid X-ray variability reported in the literature (e.g., Ricci et al. 1995; Nowak & Wilms 1999) is also consistent with the very low amplitude noise we found. The only unusual observation in our data is observation 6 for which no similar observation has been reported in the literature. Besides this observation, the behaviour of 4U 1957+11 seems to be very stable over many years as observed with several different X-ray instruments.

Nowak & Wilms (1999) claimed a 177 day period in 4U 1957+11. As shown above (§ 3.1), the long-term X-ray variability of this source is much more complicated than one single period. Also, we found that the luminosity of 4U 1957+11 can change by a factor of at least 4, which is significantly larger than what had been observed previously for this source. These variations cannot be due to changes in the column density because the high column densities ($\sim 10^{23}$ cm^{-2}) needed to account for such large luminosity fluctuations would easily have been observed in our spectra. These findings suggest that the reason behind the long-term variability is most likely not a precessing accretion disc as suggested by Nowak & Wilms (1999) but might have another cause, possibly variations in the mass accretion rate onto the compact object. This conclusion seems to confirm a recent theoretical study about precessing warped accretion discs in X-ray binaries. Ogilvie & Dubus (2001) showed that the orbital radius of 4U 1957+11 is well below the critical radius for a stable precessing accretion disc to evolve in this system. A possible mechanism for the long-term fluctuations in systems like 4U 1957+11 might be that a modulation of the accretion rate through the disc can occur when a viscously

unstable disc is irradiated by a constant X-ray flux (Ogilvie & Dubus 2001; G. Dubus 2001 private communication; see also Dubus et al. 2001 in preparation).

5.2 Comparison with neutron-star LMXBs

The behaviour displayed by 4U 1957+11 is not that typical for neutron-star LMXBs. For such neutron-star systems, the X-ray spectrum can also be described by a soft component below 3 keV and a power-law component above 10 keV. However, the power-law component becomes significantly weaker when the luminosities or the inferred mass accretion rates of these systems increase (see, e.g., Di Salvo et al. 2000 and references therein), which is completely opposite to what we observe for 4U 1957+11. It is possible that for 4U 1957+11 the mass accretion rate is anti-correlated with the X-ray luminosity as observed in the brightest neutron star LMXBs (the so-called Z sources; see Hasinger & van der Klis 1989), but we regard this possibility as unlikely. At times when the luminosity is thought to be anti-correlated with the mass accretion rate in Z sources (on their “normal branch”), the intrinsic luminosity is close to the Eddington luminosity, but 4U 1957+11 seems to be significantly weaker (the source has to be unlikely distant in order to have near-Eddington luminosities).

Also, quasi-periodic oscillations near 7 Hz and 50–60 Hz are often reported in the Z sources when they are on their normal branches together with band-limited noise which increases in strength when the source becomes harder (up to 10%–15% rms amplitude; see van der Klis 1995 for a review about the timing properties of Z sources). Such strong noise and quasi-periodic oscillations have never been observed for 4U 1957+11, despite the range in luminosities sampled and the different instruments used (Ricci et al. 1995; Nowak & Wilms 1999). We tentatively suggest that it is more likely that 4U 1957+11 harbors a black hole than a neutron star.

5.3 Comparison with black-hole X-ray binaries

It has already been noted that the soft X-ray spectrum of 4U 1957+11 resembles that of BHCs when they are in their high state (e.g., White & Marshall 1984; see Homan et al. 2001 for a recent detailed discussion of black-hole states). The very low amplitude variability observed for 4U 1957+11 is also consistent with this. Several arguments were put forward against a black-hole nature of 4U 1957+11. A main argument is that the luminosity of 4U 1957+11 is considerably lower than that of BHCs in their high state. But, as already explained above (§ 4), the distance to the source is not well known. Although the true luminosity of 4U 1957+11 could be considerably higher than the normal $5\text{--}10 \times 10^{36}$ erg s⁻¹ assumed, it could also be less. However, for several BHCs (e.g., GRO J1655–40; XTE J1550–564; Méndez, Belloni, & van der Klis 1998; Sobczak et al. 1999; Homan et al. 2001) it has been found that high state episodes can occur also in those sources at relatively low luminosities ($< 10^{37}$ erg s⁻¹). This demonstrates that the luminosity argument against 4U 1957+11 being a black hole is not well founded.

Another argument is that the obtained inner disc radius obtained from the spectral fits (several km) is too low and the temperature of the disc (~ 1.5 keV) too high to

be in agreement with what has been found for other BHCs (e.g., Yaqoob et al. 1993). However, the disc radius depends on the unknown distance and inclination of the system and they might be larger than usually assumed (see also Nowak & Wilms 1999). Disc temperatures close to those observed for 4U 1957+11 have also been observed during the high states of other BHC, such as LMC X-3 (see below) and XTE J1748–288 (Miller et al. 2001). For the enigmatic BHC GRS 1915+105 disc temperatures up to 2 keV have been observed during its high state (e.g., Rao, Yadav, & Paul 2000), although it is unclear if a comparison between 4U 1957+11 and GRS 1915+105 is really valid because of the very unusual behaviour of GRS 1915+105. However, this demonstrates that although the disc temperature of 4U 1957+11 is relatively high compared to most BHCs, it is not a compelling reason to dismiss the possibility that 4U 1957+11 contains a black hole. Especially a comparison of this source with the strong black-hole X-ray binary LMC X-3 suggests a black-hole nature for 4U 1957+11.

5.4 Comparison with LMC X-3

LMC X-3 is a strong BHC with a black-hole mass of $>5.8 M_{\odot}$ (see Soria et al. 2001 and references therein). This source is unusual in that it spends most of its time in the canonical black-hole high state although occasionally it makes excursions to the black-hole low state (see Boyd et al. 2000, Wu et al. 2001, and Wilms et al. 2001 for observations of LMC X-3 in its low state). The spectrum of LMC X-3 is very similar to that of 4U 1957+11 (although its disc temperature is at maximum only ~ 1.3 keV; Nowak et al. 2001; Wilms et al. 2001). Its spectrum hardens with increasing luminosity (Cowley et al. 1991; Ebisawa et al. 1993; Wilms et al. 2001; note that dramatic spectral hardening also occur when the source luminosity decreases considerably, thus when the source transit from its normal high state to its low state; see Boyd et al. 2000 and Wilms et al. 2001) in a way similar to what we observed for 4U 1957+11 (the hardening is mostly due to an increase of the disc temperature). And as for 4U 1957+11, hardly any variability on short time scale could be detected (e.g., Nowak et al. 2001) and the source exhibits strong long-term X-ray fluctuations (Cowley et al. 1994; Wilms et al. 2001; factor of 5 for LMC X-3 and at least 4 for 4U 1957+11). The only apparent differences between the two sources is the fact that LMC X-3 can be as bright as 10^{38} erg s⁻¹ (2–10 keV) and that 4U 1957+11 is most likely considerably weaker. As explained above (§ 4), the distance to 4U 1957+11 is not well-constrained and the source could be further away than the (usually) assumed distance of 7 kpc (Margon et al. 1978). However, this last effect might only account for a small increase in the luminosity of 4U 1957+11 because the source should be far away to have an intrinsic luminosity similar to what is usually observed from LMC X-3.

It is possible that the black-hole mass in 4U 1957+11 is considerably lower than that of the black hole in LMC X-3. If the specific accretion rate above which a black-hole X-ray binary enters the high state is tied to the mass of the black hole (e.g., such transition occurs at a fixed fraction of the critical Eddington mass accretion rate), then it will be reached earlier in 4U 1957+11 than in LMC X-3. This could explain why 4U 1957+11 is not as bright as LMC X-3. A

possible other solution might be the lower metallicity in the LMC compared to the Galaxy. This might give higher luminosities for accreting X-ray binaries (as proposed to explain the on averaged higher luminosities for the X-ray binaries in the SMC and LMC; see, e.g., Clark et al. 1978). It remains to be determined whether this could explain the luminosity difference between the two sources.

Despite this difference in intrinsic luminosity, the many similarities between these two sources suggest that, similar to LMC X-3, 4U 1957+11 harbors a black hole and the long-term fluctuations are due to changes in the mass accretion rate. If this can be proven, then 4U 1957+11 would be the only persistent Galactic BHC which is continuously observed in the black-hole high state. The other persistent galactic BHCs (e.g., Cyg X-1, 1E 1740.7–2942) are most often observed in the black-hole low state and only rarely make excursions to the high state (the other persistent BHC which spends all of its time in the black-hole high state is LMC X-1, also in the LMC, and is a wind-fed system).

Several predictions can be made if we assume that 4U 1957+11 is indeed is black-hole binary. It is possible that at very high luminosities (higher than so far observed), the source might transit to the black-hole very high state and strong quasi-periodic oscillations might be observed. At the lowest end of the luminosity range, it might be possible that the source will enter the black-hole low state and the spectrum will then considerably harden and strong rapid X-ray variability will be observed. Such a transition was recently observed for LMC X-3 (Boyd et al. 2000; Wilms et al. 2001) suggesting that such a change is also possible for 4U 1957+11. Observing either state in 4U 1957+11 would strongly confirm that this source is a BHC.

It is possible that the excursion of the source to a harder state during observation 6, can be identified with a very high state, but the weak variability of the source during this observation and the non-detections of quasi-periodic oscillations around 6 Hz does not seem to be consistent with this scenario. However, in other BHCs strong variability or quasi-periodic oscillations have not always been observed when they were at high luminosities and exhibited hard spectra. For example, for XTE J1550–564 it was observed that, when this source was relatively bright, it occasionally exhibited short excursions to hard states without a significant increase in the strength of the rapid X-ray variability (see Homan et al. 2001 and in particular the small flares discussed by these authors). Also, Wijnands et al. (2001) reported that only weak noise (less than a few percent rms amplitude) could be detected during some very-high state observations of GRS 1739–278. Therefore, it is still possible that 4U 1957+11 might have exhibited very-high state like behaviour during observation 6.

If indeed 4U 1957+11 exhibits state behaviour similar to other BHCs, then during those hard states an increase in radio luminosity is also expected and a monitoring radio campaign on the source might be able to reveal radio emission from this source at the extreme end of the luminosity range. The only radio observations of 4U 1957+11 reported so far, did not reveal any strong radio emission from the source (Nelson & Spencer 1988), however, it is unclear what the X-ray luminosity was at the time of those observations. However, our *RXTE* observations show that 4U 1957+11 spends most (if not all) of its time in the soft state and it is

likely it was in a similar state during the Nelson & Spencer (1988) observation. This would be consistent with their non-detection in the radio band, because black-hole candidates do not show strong radio emission in their soft states (e.g., Fender 2001). Note also, that null results from a monitoring radio campaign will not exclude the possibility that 4U 1957+11 is a BHC because it might well be possible that the high or low accretion rates needed for the state changes to occur are not reached in this system.

6 CONCLUSION

The conclusions obtained from our analysis of the *RXTE* data of 4U 1957+11 are:

- The X-ray luminosity of 4U 1957+11 can vary by at least a factor of 4.
- The 3–20 keV spectrum can be adequately described by a multi-colour disc black-body and a power-law component.
- The spectrum significantly hardens when the luminosity increases, both as a result of an increase of the disc temperature and, although to a lesser degree, an increase in the power-law flux contribution to the total flux.
- Only very weak variability on short time scales could be observed (of order one percent rms amplitude).
- A comparison of 4U 1957+11 with other X-ray binaries, i.e., LMC X-3, suggests that 4U 1957+11 contains a black hole and not a neutron star. The spectral and temporal properties of 4U 1957+11 indicate that the source is a black-hole LMXB persistently in the black-hole high state. If confirmed, the source would be the only such source known.
- The long-term variability of the source is highly complex and most likely due to variations in the accretion rate onto the black hole.

ACKNOWLEDGMENTS

This work was supported by NASA through Chandra Postdoctoral Fellowship grant number PF9-10010 awarded by CXC, which is operated by SAO for NASA under contract NAS8-39073. This work was also supported in part by the Netherlands Organization for Scientific research (NWO). This research has made use of data obtained through the HEASARC Online Service, provided by the NASA/GSFC and quick-look results provided by the ASM/*RXTE* team. RW thanks Guillaume Dubus for useful discussions.

REFERENCES

- Barret, D. & Vedrenne, G. 1994, *ApJS*, 92, 505
 Barret, D., McClintock, J. E., Grindlay, J. E. 1996, *ApJ*, 473, 963
 Belloni, T., Klein-Wolt, M., Méndez, M., van der Klis, M., van Paradijs, J. 2000, *A&A*, 355, 271
 Boyd, P. T., Smale, A. P., Homan, J., Jonker, P. G., van der Klis, M., Kuulkers, E. 2000, *ApJ* 542, L127
 Bradshaw, C. F., Fomalont, E. B., & Geldzahler, B. J. 1999, *ApJ*, 512, L121
 Christian, D. J. & Swank, J. H. 1997, *ApJS*, 109, 177
 Clark, G., Doxsey, R., Li, F., Jernigan, J. G., van Paradijs, J. 1978, *ApJ*, 221, L37

- Cowley, A. P., Schmidtke, P. C., Ebisawa, K., Makino, F., Remillard, R. A., Crampton, D., Hutchings, J. B., Kitamoto, S., Treves, A. 1991, *ApJ*, 381, 526
- Cowley, A. P., Schmidtke, P. C., Hutchings, J. B., Crampton, D. 1994, *ApJ*, 429, 826
- Dickey, J. M. & Lockman, F. J. 1990, *ARAA*, 28, 215
- Di Salvo, T., Stella, L., Robba, N. R., van der Klis, M., Burderi, L., Israel, G. L., Homan, J., Campana, S., Frontera, F., Parmar, A. N. 2000, *ApJ*, 544, L119
- Ebisawa, K., Makino, F., Mitsuda, K., Belloni, T., Cowley, A. P., Schmidtke, P. C., Treves, A. 1993, *ApJ*, 403, 684
- Fender, R. 2001, To appear in "Relativistic flows in Astrophysics", Springer Verlag Lecture Notes in Physics, Eds A.W. Guthmann, M. Georganopoulos, K. Manolakou and A. Marcowith (astro-ph/0109502)
- Filippenko, A. V., Leonard, D. C., Matheson, T., Li, W., Moran, E. C., Riess, A. G. 1999, *PASP*, 111, 969
- Hakala, P. J., Muhli, P., Dubus, G. 2000, *MNRAS*, 306, 701
- Hasinger, G. & van der Klis M. 1989, *A&A*, 225, 79
- Homan, J., Wijnands, R., van der Klis, M., Belloni, T., van Paradijs, J., Klein-Wolt, M., Fender, R., Méndez, M. 2001, *ApJS* 132, 377
- Levine, A. M., Bradt, H., Cui, W., Jernigan, J. G., Morgan, E. H., Remillard, R., Shirey, R. E., Smith, D. A. 1996, *ApJ*, 469, L33
- Liu, Q.Z., van Paradijs, J., van den Heuvel, E., 2001, *A&A* 368, 1021
- Lomb, N. R. 1976, *Ap&SS*, 39, 447
- Margon, B., Thorstensen, J. R., & Bowyer, S. 1978, *ApJ*, 221, 907
- McClintock, J. E., Garcia, M. R., Caldwell, N., Falco, E. E., Garnavich, P. M., Zhao, P. 2001, *ApJ*, 551, L147
- Méndez, M., Belloni, T., & van der Klis M. 1998, *ApJ*, 499, L187
- Miller, J. M., Fox, D. W., Di Matteo, T., Wijnands, R., Belloni, T., Pooley, D., Kouveliotou, C., Lewin, W. H. G. 2001, *ApJ*, 546, 1055
- Nelso, R. F. & Spencer, R. E. 1988, *MNRAS*, 234, 1105
- Nowak, M. A. & Wilms, J. 1999, *ApJ*, 522, 476
- Nowak, M. A., Wilms, J., Heindl, W. A., Pottschmidt, K., Dove, J. B., Begelman, M. C. 2001, *MNRAS*, 320, 316
- Ogilvie, G. I. & Dubus, G. 2001, *MNRAS*, 320, 485
- Rao, A. R., Yadav, J. S., & Paul, B. 2000, *ApJ*, 544, 433
- Ricci, D., Israel, G. L., Stella, L. 1995, *A&A*, 299, 731
- Scargle, J. D. 1982, *ApJ*, 263, 835
- Singh, K. P., Apparao, K. M. V., Kraft, R. 1994, *ApJ*, 421, 753
- Sobczak, G. J., McClintock, J. E., Remillard, R. A., Bailyn, C. D., Orosz, J. A. 1999, *ApJ*, 520, 776
- Soria, R., Wu, K., Page, M. J., Sakelliou, I. 2001, *A&A*, 365, L273
- Thorstensen, J. R. 1987, *ApJ*, 312, 739
- van der Klis, M. 1994a, *A&A*, 283, 469
- van der Klis, M. 1994b, *ApJS*, 92, 511
- van der Klis, M. 1995, Ch. 6 in: "X-ray Binaries", eds. Lewin et al., Cambridge Univ. Press. p. 252
- van Paradijs, J. 1995, Ch. 14 in: "X-ray Binaries", eds. Lewin et al., Cambridge Univ. Press. p. 536
- White, N. & Marshall, F. E. 1984, *ApJ*, 281, 354
- Wijnands, R. & van der Klis, M. 1999, *ApJ*, 514, 939
- Wijnands, R., Méndez, M., Miller, J. M., Homan, J. 2001, *MNRAS*, 328, 451
- Wilms, J., Nowak, M. A., Pottschmidt, K., Heindl, W. A., Dove, J. B., Begelman, M. C. 2001, *MNRAS*, 320, 327
- Wu, K., Soria, R., Page, M. J., Sakelliou, I., Kahn, S. M., de Vries, C. P. 2001, *A&A* 365, L267
- Yaqoob, T., Ebisawa, K., Mitsuda, K. 1993, *MNRAS*, 264, 411

Table 1. Log of the observations

Number	Observation ID	Observation time (UTC)	Good time (ksec)	PCUs on	Count rate ^a (counts s ⁻¹ PCU ⁻¹)	Count rate range ^b (counts s ⁻¹ PCU ⁻¹)
AO2 observations						
	20184- ^c		29.2		48.1±0.05	41.7–54.1
1	01-01-000	1997 Nov 26 00:23–07:45	15.5	All	48.4±0.1	42.7–54.1
2	01-01-00	1997 Nov 26 08:23–10:44	6.2	All	48.1±0.1	43.0–52.7
3	01-01-01	1997 Nov 27 01:59–04:05	4.7	All	47.4±0.1	41.7–53.1
4	01-01-02	1997 Nov 29 02:00–02:48	2.8 ^d	All/1,2,3,4 ^d	48.2±0.1	43.9–53.4
AO4 observations						
	40044- ^c		38.6		105.6±0.05	69.8–171.
5	01-01-00	1999 March 03 02:33–03:19	2.7	All	105.6±0.1	96.9–116.5
6	01-02-01 ^e	1999 April 03 10:43–12:42	3.9	All		
6a	Rise	1999 April 03 10:43–11:06	1.3		101.1±0.2	83.7–123.6
6b	Plateau	1999 April 03 11:43–12:42	2.6		160.9±0.2	150.8–171.4
7	01-02-00	1999 April 06 23:01–23:50	3.0	0,2,3	131.2±0.2	118.4–144.9
8	01-03-02	1999 April 17 03:41–04:28	2.8	0,1,2	86.7±0.1	89.2–93.8
9	01-03-03	1999 April 17 05:18–05:54	2.2	0,2	86.7±0.2	76.1–94.7
10	01-03-00	1999 April 20 21:03–21:45	2.5	0,2,4	86.5±0.2	76.5–95.6
11	01-03-01	1999 April 21–22 23:25–01:11	3.9	0,2,3,4	90.3±0.2	83.1–101.1
12	01-04-00	1999 May 04 18:12–21:45	8.1	0,2,3,4	81.5±0.1	69.8–92.0
13	02-01-02	1999 Dec 01 23:05–23:42	2.2	All	126.0±0.2	117.5–136.0
14	02-01-01	1999 Dec 02 00:39–01:24	2.6	All	128.8±0.2	118.6–144.0
15	02-01-00	1999 Dec 02 02:15–04:19	4.7	All	121.9±0.2	109.7–138.9

^a Averaged, background subtracted count rate per ObsID for the nominal *RXTE*/PCA energy range of 2–60 keV (all 129 energy channels for the Standard 2 mode data). The error bars on the count rates are statistical errors.

^b The range of count rates observed for each observation.

^c All observations with this ObsID combined

^d 1.5 ksec with all PCUs on and 1.3 ksec with only PCUs 1–4 on

^e Significant increase in the count rate observed during the observation

Table 2. VLFN parameters versus count rate

Average count rate ^a (counts s ⁻¹ PCU ⁻¹)	Amplitude ^b (% rms)	Index	Observations combined
101 ⁺²³ ₋₁₇	6.0 ^{+0.7} _{-0.6}	0.7±0.1	6a
160±11	<1.1	1.5 ^c	6b
48±6	1.3±0.1	1.8±0.3	1–4
85±16	1.4 ^{+0.2} _{-0.1}	2.1 ^{+0.4} _{-0.3}	8–12
106 ⁺¹¹ ₋₉	1.7±0.3	1.5±0.4	5
126±18	2.2±0.1	1.35±0.09	7, 13–15

^a For the total 2–60 keV *RXTE*/PCA energy range. The errors are the range of count rates observed during the observations which were combined.

The count rates are background subtracted.

^b Measured for the frequency range 0.001–10 Hz

^c Index fixed

Table 3. X-ray spectral parameters^a

Number	T_{disc} (keV)	$Norm_{disc}$	F_{disc}^b	Γ	$Norm_{pl}$ ($\times 10^{-2}$)	F_{pl}^b	Width (keV)	$Norm_{line}$ ($\times 10^{-4}$)	EW (eV)	F_{line}^b	F_{tot}^c
1	1.33±0.01	15.6±0.30	4.1±0.1	2.5 ^d	<0.13	<0.015	0.8±0.2	4.1±0.7	107±18	4.3±0.8	4.2 ^{+0.4} _{-0.3}
2	1.31±0.01	15.9 ^{+0.4} _{-0.3}	3.9±0.1	2.5 ^d	1.4 ^{+0.1} _{-0.2}	0.16 ^{+0.01} _{-0.02}	1.0±0.2	5.2±0.9	136±22	5.4±0.9	4.1±0.3
3	1.33±0.01	15.6±0.4	4.1±0.1	2.5 ^d	<0.10	<0.011	0.6 ^{+0.2} _{-0.3}	3.7±0.8	98±21	3.8±0.9	4.2±0.3
4	1.34±0.01	15.0 ^{+0.2} _{-0.1}	4.2 ^{+0.2} _{-0.1}	2.5 ^d	<0.37	<0.042	0.8 ^{+0.7} _{-0.8}	2.3 ^{+4.4} _{-2.0}	57 ⁺¹¹² ₋₄₉	2.5 ^{+4.5} _{-2.2}	4.2 ^{+0.3} _{-0.2}
5	1.55±0.01	14.4±0.3	8.3 ^{+0.1} _{-0.2}	2.32 ^{+0.05} _{-0.06}	8.9±1.2	1.4±0.2	0.9±0.5	6.4±2.2	65±22	6.5±2.1	9.9 ^{+0.5} _{-0.7}
6a	1.64±0.02	4.0±0.3	3.1±0.2	2.42 ^{+0.01} _{-0.02}	52.4±1.7	7.0 ^{+0.2} _{-0.3}	0.4 ^{+0.5} _{-0.4}	4.8±2.1	53±24	5.0±2.2	10.2±0.5
6b	1.82 ^{+0.02} _{-0.01}	5.8±0.2	7.6±0.3	2.34 ^{+0.01} _{-0.02}	54.9±1.8	8.5±0.3	0.3 ^{+0.6} _{-0.3}	5.8 ^{+3.1} _{-2.7}	40±20	6.0 ^{+3.2} _{-2.8}	16.2±0.6
7	1.63±0.01	14.6±0.3	10.8±0.2	2.3±0.1	6.8 ^{+1.7} _{-1.4}	1.1 ^{+0.3} _{-0.2}	0.8±0.3	9.9±2.7	79±22	10.3±2.8	12.2±0.6
8	1.48±0.01	15.3 ^{+0.4} _{-0.5}	7.2 ^{+0.1} _{-0.3}	2.3±0.4	1.6 ^{+1.9} _{-0.9}	0.3 ^{+0.3} _{-0.2}	0.5 ^{+1.0} _{-0.5}	3.6 ^{+2.2} _{-1.7}	48 ⁺²⁹ ₋₂₃	3.7 ^{+2.3} _{-1.7}	7.4±0.5
9	1.46±0.01	15.8±0.5	6.9 ^{+0.2} _{-0.3}	2.7±0.2	6.6 ^{+3.2} _{-2.3}	0.5±0.2	1.4±0.3	11.6 ^{+2.0} _{-2.4}	158 ⁺²⁹ ₋₃₃	12.0 ^{+2.1} _{-2.5}	7.5 ^{+0.6} _{-0.5}
10	1.51±0.01	11.3±0.4	5.8±0.2	2.94±0.04	44.4 ^{+4.3} _{-3.6}	2.2±0.2	0.3 ^{+0.4} _{-0.3}	3.7±1.7	48±22	3.8±1.7	8.1 ^{+0.5} _{-0.3}
11	1.48±0.01	15.1±0.4	6.9±0.2	2.48±0.06	11.5 ^{+1.7} _{-1.4}	1.3 ^{+0.3} _{-0.1}	0.9±0.3	8.1±1.8	100±22	8.4±1.9	8.4 ^{+0.3} _{-0.8}
12	1.48±0.01	15.4±0.1	7.0±0.1	2.4±0.3	1.5 ^{+1.4} _{-0.7}	0.2 ^{+0.2} _{-0.1}	0.6±0.3	4.7±1.4	64±19	4.9±1.5	7.4±0.3
13	1.59±0.01	13.0 ^{+0.3} _{-0.4}	8.6 ^{+0.2} _{-0.3}	2.41 ^{+0.04} _{-0.03}	24.1±2.3	3.2 ^{+0.3} _{-0.2}	0.8±0.5	7.0±2.6	60±22	7.3±2.7	12.0 ^{+0.5} _{-0.7}
14	1.57±0.01	15.7 ^{+0.3} _{-0.4}	9.8 ^{+0.2} _{-0.4}	2.17±0.05	9.2±1.2	2.0 ^{+0.2} _{-0.3}	1.0±0.3	10.9±2.7	91±23	11.3±2.8	11.9±0.6
15	1.57±0.01	14.8±0.3	9.3±0.2	2.75±0.06	21.3±3.0	1.5±0.2	0.9±0.2	13.9±2.3	126±22	14.4±2.4	10.9 ^{+0.6} _{-0.5}

^a The column density was fixed to 1.3×10^{21} atoms cm^{-2} , the errors are for 90% confidence levels, the centroid energy of the line was fixed at 6.5 keV, and the reduced χ^2 of the fits were below 1 except for observations 1 and 2 where they were ~ 1.7 .

^b Fluxes are for 3–20 keV, absorbed, and in units of 10^{-10} erg s^{-1} cm^{-2} for the MCD and power law component and in 10^{-12} erg s^{-1} cm^{-2} for the line

^c Total fluxes are for 3–20 keV, unabsorbed, and in units of 10^{-10} erg s^{-1} cm^{-2}

^d Parameter fixed